WILEY-VCH

# Biomimicking stretchable organic electrochemical transistor

*Yuanzhe Li, Naixiang Wang, Anneng Yang, Haifeng Ling, Feng Yan**

Mr. Y. Li, Dr. N. Wang, Mr. A. Yang, Dr. H. Ling, Prof. F. Yan
Department of Applied Physics
The Hong Kong Polytechnic University
Hong Kong, China
E-mail: apafyan@polyu.edu.hk

**Keywords:** organic electrochemical transistor, flexible electronics, biomimicking, glucose detection

## Abstract

Stretchable organic electrochemical transistors (OECTs) can find applications in wearable electronics for biosensing. However, the existing fabrication method is either inconvenient or expensive. Here, we report a novel method to fabricate stretchable OECTs based on biomimicking polydimethylsiloxane substrates. The substrate pattern is transferred from the bract of bougainvillea glabra, demonstrating a 2-dimensional wavy structure. To further enhance the stretchability of the Au electrodes of the devices on the wavy surface, we coat a highly conductive polymer film on the Au surface by inkjet printing to bridge disconnected parts separated by cracks. The obtained OECTs demonstrate omnidirectional stretchability up to 30% and bending radius down to 15 mm with stable performance. Stretchable glucose sensors with a detection limit around 1 μM are developed based on the biomimicking stretchable OECTs, which are sensitive enough for detecting glucose levels in body fluids.

## 1. Introduction

Organic thin film transistors, including organic field effect transistors (OFETs) and organic electrochemical transistors (OECTs), have attracted much attention in recent years for their promising applications in flexible and wearable electronics.[1-3] Compared to OFETs, OECTs can be operated at low voltage (<1 V) in an aqueous environment, making them good candidates for biosensors.[4-6] Being potentiometric transducers, functionalized OECTs can detect various kinds of analytes ranging from simple ions[7], metabolites like glucose[8], lactate[9], cortisol[10], more complicated biomolecules such as DNA[11], protein[12], cells[13] and bacteria[14]. In order to better conform to and collect signals from a human body in wearable electronic systems, much efforts have been devoted to the study of flexible and stretchable biosensors. As organic semiconductors are inherently flexible, OECTs have been successfully developed for such applications in recent years,[15-17] yet there are some challenges in preparing stretchable OECTs.

A stretchable OECT includes several key elements, including substrate, electrodes and organic channel. Commonly used polydimethylsiloxane (PDMS) substrates are stretchable and some organic semiconductors can sustain around 10% strain if processed under tuned conditions[18], while metal electrodes are not stretchable. For instance, the gold film can be quickly broken over a strain of only 0.46%.[19] Although the patterning of gold electrodes into serpentine shapes can alleviate the strain,[20, 21] the fabrication process becomes more complicated. On the other hand, although there are several reports of intrinsically stretchable conductive polymers,[22-24] most of them don't fit well with existing processing technologies. Structure engineering based on commercially available materials such as PEDOT:PSS is still needed for fabricating high-performance stretchable OECTs. Zhang et al.[25] used the strategy of prestraining to neutralize deformations. Wrinkles can be generated upon the relaxation of prestrained substrate. The device prepared by this method can have uniaxial stretchability of 30%. However, complicated orthogonal

photolithography was developed to replace conventional photolithography. Moreover, compressibility was sacrificed for achieving high stretchability by the employment of prestraining.[26]

In this work, we present a novel method to fabricate stretchable OECTs based on biomimicking PDMS substrates. The substrate pattern is transferred from the bract of bougainvillea glabra, demonstrating 2-dimensional wavy structures. We find that the substrates with prefabricated wavy structures can provide device-level omnidirectional stretchability without prestraining.[26, 27] While 2-dimensional wavy structures can be achieved with prestraining in some electronic devices[32], as far as we know, there has been no report in the field of stretchable OECTs. To further enhance the stretchability of the Au electrodes on the wavy surface, we coat highly conductive PEDOT:PSS film on Au surface by inkjet printing to bridge disconnected parts separated by cracks. The obtained OECTs demonstrate omnidirectional stretchability up to 30% and bending radius down to 15 mm with stable performance. Stretchable glucose sensors with a detection limit around 1 μM are developed based on this biomimicking stretchable OECT, which are sensitive for detecting glucose levels of body fluids.

## 2. Results and Discussion

We prepared biomimicking PDMS substrates by soft lithography, which are a key element for our stretchable OECTs. Bract of bougainvillea glabra (**Figure 1**a) was first taped onto the bottom of a plastic petri dish in order to flatten the bract surface. PDMS was poured over the bract mold and later vacuum-degassed for 5 minutes to remove the bubbles. The curing condition was 48 hours at room temperature. Finally, we peeled PDMS from the mold and removed bract residues with ethanol. The thicknesses of the biomimicking substrates were around 1mm.

**Figure 1**b **and 1**d show the surface morphology of bougainvillea glabra bract. The bract

surface was highly rough and composed of buckled structures in sizes of 40-80 μm. The contoured surface was replicated to PDMS using soft lithography (**Figure 1**c **and 1**e). Since the original pattern of bract was isotropic in nature, fabricated PDMS automatically inherited the 2-dimensional wavy structures, which could be helpful in constructing omnidirectionally stretchable electronic devices. The cross section of a randomly cut biomimicking PDMS is shown in Figure 1f and the surface can be depicted with a sine function of $y= A_0\sin(2x\pi/\lambda)$, where $A_0$ is half of the peak to valley amplitude and $\lambda$ is the wavelength. The ratio of $A_0/\lambda$ is an important structure parameter and can help estimate the theoretical device stretchability. The average value was estimated to be 0.13.

The procedure for device fabrication is schematically illustrated in **Figure 2**a. After obtaining biomimicking PDMS substrates, Au/Cr electrodes were deposited on PDMS by magnetic sputtering assisted with a shadow mask. The electrode thickness was controlled to be around 100 nm by tuning the deposition time. Afterward, a PEDOT:PSS layer was printed by an inkjet printer, with a drop spacing of 20 μm and a substrate temperature of 50 ℃. Since PDMS is highly hydrophobic, the substrate was plasma-processed and fluoroadditive Zonyl was added into ink to decrease the contact angle from 72° to 30° (see supporting information **Figure S1**). In addition to the channel, PEDOT:PSS was also printed on Au electrodes to function as alternative conductive paths when cracks are generated in the Au electrodes . As the last step of functionalization, Pt flakes, glucose oxidase (GOx) and chitosan were drop cast over the gate electrodes and dried in a fridge under 4 ℃.

Inkjet printing instead of photolithography was selected here for its advantages of high throughput and the low requirement on substrate morphology. Belonging to additive manufacturing, it can accomplish depositing and patterning simultaneously by dropping ink onto desired positions. Therefore, it can facilitate the fabrication processing and save the cost. Besides, by means of inkjet printing, a uniform film can be formed even on a highly rough surface, for instance, biomimicking

PDMS.

**Figure 2**b shows that the device can be easily stretched under a strain. An increasing strain was applied onto the device in the horizontal direction and the device morphology was observed under a microscopy. With the help of the wavy substrate, the Au electrodes of biomimicking device can now survive a strain of 20% and show little cracks under strains up to 30%, as shown in **Figure 2**c. The good stretchability can also be witnessed for the polymer channel. As the control group, a conventional OECT was prepared on a planar PDMS substrate using the same processing method. Large cracks in Au electrodes of the control device can be witnessed starting from 5% strain. The cracking of PEDOT:PSS was postponed until 20% since the intrinsic tangled structure of polymer relaxed parts of strains. We noticed that the performance of the control device shows a poor stability and a small strain of 5% causes a significant degradation and 20 % strain disables the whole device (supporting information **Figure S2**) while the device on the biomimicking substrate shows much better stability under strains, which is to be introduced in the following part. This result clearly indicates that wavy surface can substantially release stains in the devices.

The reason why wavy structures can improve stretchability is due to the alleviation of the actual strain applied on the electrodes. An analytical model for the flexible system has been developed by Xiao et al.[19] For a stiff (the plane strain modulus of Au $\bar{E_f}$ >> the plane strain modulus of PDMS $\bar{E_S}$) and thin (the thin film thickness $h$ << the amplitude of sinuous structure $A_0$) Au film on a sinuous stretchable substrate, the maximum strain $\varepsilon_{max}$ applied on the Au thin film under a substrate strain $\varepsilon_a$ has the following relationship: [19]

$$\varepsilon_{max} = \varepsilon_a \frac{3\bar{E}_S\left(2-k^2{A_0}^2+k^2A_0h\right)+\bar{E}_fk^3h^2(6A_0+h)}{6\bar{E}_S+\bar{E}_fk^3h(6A_0+h)}, \quad (1)$$

where $\varepsilon_a$ the uniaxial strain applied to the PDMS substrate, $\bar{E_S}$ the plane strain modulus of PDMS, $\bar{E_f}$ the plane strain modulus of gold, $v_S$ the Poisson's ratio of PDMS, $v_f$ the Poisson's ratio of gold,

$A_0$ the amplitude of sinuous structure, $h$ the thin film thickness, $k=2\pi/\lambda$. In the case of our device, the structure parameters are $A_0/h$ = 300, $A_0/\lambda$ = 0.13, therefore $\varepsilon_a/\varepsilon_{max}$ is estimated to be 76. Crack happens when $\varepsilon_{max}$ reaches the failure strain of the Au thin film, which is 0.46% for Au. The theoretical system stretchability can then be calculated to be 35 %. However, for biomimicking device, cracking of electrodes could be witnessed under strain of 30% (**Figure 2**c). The lower value of our strain tolerance than the theoretical limit stems from two possible reasons. First, the surface pattern of bract was not uniform and in a certain direction, the wavy structure deviated from the average value. Second, impurity particles on the substrate left small pinholes on Au film. These geometric discontinuities could cause higher local stress and lead to early failure of gold material. Although the uniformity of bract cannot be guaranteed, certain strategies can be employed to eliminate the influence of the early cracking caused by stress concentration.

To further enhance the stretching and bending stability of the device, highly conductive PEDOT:PSS was ink-jet printed on Au electrodes of the devices (**Figure 3**b) and formed an Au/PEDOT:PSS bilayer structure of the electrodes. **Figure 3**a **and 3**b compare the structures of normal and enhanced biomimicking stretchable OECTs. The main difference is whether there is a PEDOT:PSS layer coated on gold electrodes.

The transfer characteristics of the devices under different strains are presented in **Figure 3**c-f**.** For the normal device without PEDOT:PSS on Au electrodes(**Figure 3**c **and 3**e), the channel current dropped significantly under increasing strain. This is attributed to that fact that cracks are generated in Au electrodes and decrease the conductivity of the electrodes. If we define the stretchability as the maximum value where the device maintains 90% of its original performance,[28] the value can be extracts as 20% strain for horizontal and 10% strain for vertical. The worse performance under vertical compared to horizontal strains can be explained by anisotropy in device dimensions because the horizontal size of the device is shorter than its vertical counterpart. Since

crack propagates normal to the direction of strains (indicated by dashed lines in figures), vertical strains are more likely to cause horizontal cracks that cut through the narrow neck of gold electrodes and damage the device more seriously.

For the enhanced device with PEDOT:PSS on Au electrodes (**Figure 3**d **and 3**f), the channel current barely changed under the horizontal strain of 30%. The stretchability in the vertical direction was worse, with the maximum tolerant strain of around 20%. The improved performance compared to normal device stemmed from the additional coating of a highly conductive PEDOT:PSS layer on Au electrodes. Since polymers are intrinsically stretchable to some degree, they can usually survive larger strains compared to Au. Coating conductive polymers on electrodes can provide an alternative conductive path bridging disconnected Au pieces. The improvement can also be witnessed in bending stability (supporting information **Figure S3**). Using the definition similar to stretchability (90% performance at zero $V_{GS}$), the bending stability is maintained under the bending radius of 45 mm for the control group. As comparison, the normal biomimicking OECT could bear curvature radius of 20 mm, and for the enhanced device, the value is 15 mm.

One of the most promising applications of stretchable electronics is wearable devices and stretchable OECTs can function as biosensors for health monitoring. As a demonstration of our biomimicking OECTs for potential body fluid sensors, we developed an attachable and stretchable glucose sensor. Glucose is an important metabolite in a human body and abnormal change of glucose concentrations in blood or body fluids can be indicators of diseases like diabetes mellitus.[29] Conventional sensing methods require blood samples, which are painful and cause infection risks. With the high sensitivity of our OECT-based glucose sensors, non-invasive detection of glucose can be developed.

Based on biomimicking OECTs, the stretchable glucose sensor we developed can be attached on different regions of human hands (**Figure 4**a). The phosphate buffered saline (PBS, pH 7.2)

solution was used as the electrolyte. The hand movement was simulated by imposing equivalent strains within a device and the biomimicking OECT could work stably under the condition as shown in **Figure 4**b.

The working principle for sensing glucose using our biomimicking OECTs is similar to the works reported previously.[8, 30] Two main reactions occurred with the addition of glucose:

$$D-\text{glucose} \xrightarrow{\text{GOx}} D-\text{glucono}-1,5-\text{lactone}+H_2O_2 \quad (2)$$

$$H_2O_2 \xrightarrow{\text{Pt}} O_2+2\text{e} \quad . \quad (3)$$

The enzyme glucose oxidase (GOx) immobilized on the gate electrode catalyzed glucose into $H_2O_2$ and $H_2O_2$ was later decomposed by Pt and caused an effective gate voltage shift according to the Nernst equation:[8]

$$\Delta V_{H_2O_2} \propto \frac{kT}{2q} ln[H_2O_2] \quad , \quad (4)$$

where $k$ is Boltzman constant, $T$ the temperature and $[H_2O_2]$ the concentration of $H_2O_2$. The response can therefore be read out as channel current change.

The current response of the biomimicking OECT to glucose of different concentrations is demonstrated in **Figure 4**c. The measured effective voltage change versus glucose concentration is shown in **Figure 4**d. The detection limit of our biomimicking device for glucose can be down to 1 μM. Considering the glucose concentration in a human body fluid is usually in the range of 10-200 μM,[31] biomimicking OECT is fully qualified for use in future body fluid detection.

## 3. Conclusions

By making use of bracts from bougainvillea glabra, we fabricated stretchable OECTs on the biomimicking PDMS substrates. High-throughput and low-cost inkjet printing was employed to replace photolithography. Deformations were relieved by 2-dimensional wavy structures on PDMS.

In order to further improve the stretchability, PEDOT:PSS were coated on the Au electrodes, which can eliminate the effect of cracks by bridging disconnected parts in Au electrodes. The resulting device could maintain stable performance under an omnidirectional strain up to 30 % and a bending radius down to 15 mm. An attachable glucose sensor was also developed based on this device and achieved detection limit down to 1 μM. This work presents a new method to fabricate stretchable OECT and paves way for future application of OECT as wearable devices for body fluid sensing.

## 4. Experimental Section

PDMS (Sylgard 184) is purchased from TaoDu Technology Co. The mixing ratio of base and curing agent is 15:1 for PDMS. Bougainvillea glabra was collected freshly on campus. PEDOT:PSS aqueous solution (PH500, 1g/ml) was purchased from Sigma-Aldrich Co. The PEDOT:PSS ink used for inkjet printing was composed of 90% PEDOT:PSS, 5% glycerin and 5% Zonyl fluor-surfactant (diluted to 10% in advance). The ink was then stirred for 15 min and filtered by a 0.45 um nylon filter before being injected into the cartridge. The glycerin improves the conductivity of formed PEDOT:PSS film and increases the boiling point of ink, effectively easing the clogging of nozzles during printing. Zonyl fluoroadditive enhances the adhesion of PEDOT:PSS on hydrophobic PDMS substrate. Pt flakes were recycled from lifting off process and ultrasonicated into flakes. Glucose oxidase (GOx) (50 kU/g) was purchased from Aladdin Reagent Database Inc. GOx solution was prepared by dissolving in phosphate buffered saline (PBS, pH 7.2, Invitrogen Inc. ) at a concentration of 5mg/ml. Chitosan (CHIT) solution (5mg/ml) was obtained by dissolving CHIT in acetic acid solution. De-ionized (DI) water was used throughout the experiment.

The piezoelectric inkjet printer (Dimatix, DMP 2831) coupled with a 10 pL cartridge was used to print PEDOT:PSS. The contact angle of different substrates was characterized by contact angle

212 measurement with the help of a video contact-angle analyzer. Optical microscopy (OM) and
213 electron scanning microscopy (SEM) were used to investigate the morphology of the bract and
214 PDMS substrate. All electronic measurements were carried out with Keithley 2400 sourcemeters
215 and controlled by computer software.

## Supporting Information

Supporting Information is available from the Wiley Online Library or from the author.

## Acknowledgements

This work is financially supported by the Research Grants Council (RGC) of Hong Kong, China (Project No. C5015-15G), the Innovation and Technology Commission of Hong Kong (Project No. MRP/040/18X), and the Hong Kong Polytechnic University (Project No. G-YBJ0 and G-UAF1)

## Conflict of Interest

The authors declare no conflict of interest

Received: ((will be filled in by the editorial staff))
Revised: ((will be filled in by the editorial staff))
Published online: ((will be filled in by the editorial staff))

## References


[1] W. Gao, S. Emaminejad, H. Y. Y. Nyein, S. Challa, K. Chen, A. Peck, H. M. Fahad, H. Ota, H. Shiraki, D. Kiriya, *Nature* **2016**, *529*, 509.

[2] J. Kang, D. Son, G. J. N. Wang, Y. Liu, J. Lopez, Y. Kim, J. Y. Oh, T. Katsumata, J. Mun, Y. Lee, *Adv. Mater.* **2018**, *30*, 1706846.

[3] S. Wang, J. Xu, W. Wang, G.-J. N. Wang, R. Rastak, F. Molina-Lopez, J. W. Chung, S. Niu, V. R. Feig, J. Lopez, *Nature* **2018**, *555*, 83.

[4] N. Wang, A. Yang, Y. Fu, Y. Li, F. Yan, *Acc. Chem. Res.* **2019**, *52*, 277.

[5] H. Ling, S. Liu, Z. Zheng, F. Yan, *Small Methods* **2018**, *2*, 1800070.

[6] J. Rivnay, S. Inal, A. Salleo, R. M. Owens, M. Berggren, G. G. Malliaras, *Nat. Rev. Mater.* **2018**, *3*, 17086.

[7] M. Sessolo, J. Rivnay, E. Bandiello, G. G. Malliaras, H. J. Bolink, *Adv. Mater.* **2014**, *26*, 4803.

[8] H. Tang, F. Yan, P. Lin, J. Xu, H. L. Chan, *Adv. Funct. Mater.* **2011**, *21*, 2264.

[9] D. Khodagholy, V. F. Curto, K. J. Fraser, M. Gurfinkel, R. Byrne, D. Diamond, G. G. Malliaras, F. Benito-Lopez, R. M. Owens, *J. Mater. Chem.* **2012**, *22*, 4440.

[10] O. Parlak, S. T. Keene, A. Marais, V. F. Curto, A. Salleo, *Sci. Adv.* **2018**, *4*, eaar2904.

[11] P. Lin, X. Luo, I. M. Hsing, F. Yan, *Adv. Mater.* **2011**, *23*, 4035.

[12] Y. Fu, N. Wang, A. Yang, H. K. w. Law, L. Li, F. Yan, *Adv. Mater.* **2017**, *29*, 1703787.

[13] P. Lin, F. Yan, J. Yu, H. L. Chan, M. Yang, *Adv. Mater.* **2010**, *22*, 3655.

[14] R.-X. He, M. Zhang, F. Tan, P. H. Leung, X.-Z. Zhao, H. L. Chan, M. Yang, F. Yan, *J. Mater. Chem.* **2012**, *22*, 22072.

[15] C. Liao, C. Mak, M. Zhang, H. L. Chan, F. Yan, *Adv. Mater.* **2015**, *27*, 676.

[16] J. Rivnay, P. Leleux, M. Ferro, M. Sessolo, A. Williamson, D. A. Koutsouras, D. Khodagholy, M. Ramuz, X. Strakosas, R. M. Owens, *Sci. Adv.* **2015**, *1*, e1400251.

[17] A. Yang, Y. Li, C. Yang, Y. Fu, N. Wang, L. Li, F. Yan, *Adv. Mater.* **2018**, *30*, 1800051.

[18] S. Zhang, Y. Li, G. Tomasello, M. Anthonisen, X. Li, M. Mazzeo, A. Genco, P. Grutter, F. Cicoira, *Adv. Electron. Mater.* **2019**, 1900191.

[19] T. Weihs, S. Hong, J. Bravman, W. Nix, *J. Mater. Res.* **1988**, *3*, 931.

[20] B. Marchiori, R. Delattre, S. Hannah, S. Blayac, M. Ramuz, *Sci. Rep.* **2018**, *8*, 8477.

[21] W. Lee, S. Kobayashi, M. Nagase, Y. Jimbo, I. Saito, Y. Inoue, T. Yambe, M. Sekino, G. G. Malliaras, T. Yokota, *Sci. Adv.* **2018**, *4*, eaau2426.

[22] N. Matsuhisa, M. Kaltenbrunner, T. Yokota, H. Jinno, K. Kuribara, T. Sekitani, T. Someya, *Nat. Commun.* **2015**, *6*, ncomms8461.

[23] J. Xu, S. Wang, G.-J. N. Wang, C. Zhu, S. Luo, L. Jin, X. Gu, S. Chen, V. R. Feig, J. W. To, *Science* **2017**, *355*, 59.

[24] J. Y. Oh, S. Rondeau-Gagné, Y.-C. Chiu, A. Chortos, F. Lissel, G.-J. N. Wang, B. C. Schroeder, T. Kurosawa, J. Lopez, T. Katsumata, *Nature* **2016**, *539*, 411.

[25] S. Zhang, E. Hubis, G. Tomasello, G. Soliveri, P. Kumar, F. Cicoira, *Chem. Mater.* **2017**, *29*, 3126.

[26] J. Xiao, A. Carlson, Z. Liu, Y. Huang, H. Jiang, J. A. Rogers, *Appl. Phys. Lett.* **2008**, *93*, 013109.

[27] R. Guo, Y. Yu, J. Zeng, X. Liu, X. Zhou, L. Niu, T. Gao, K. Li, Y. Yang, F. Zhou, *Adv. Sci.* **2015**, *2*, 1400021.

[28] Y. Zhu, N. Li, T. Lv, Y. Yao, H. Peng, J. Shi, S. Cao, T. Chen, *J. Mater. Chem. A* **2018**, *6*, 941.

[29] A. Heller, B. Feldman, *Chem. Rev.* **2008**, *108*, 2482.

[30] C. Liao, M. Zhang, L. Niu, Z. Zheng, F. Yan, *J. Mater. Chem. B* **2013**, *1*, 3820.

[31] M. Bariya, H. Y. Y. Nyein, A. Javey, *Nat. Electron.* **2018**, *1*, 160.

[32] D. H. Kim, J. A. Rogers, *Adv. Mater.* **2010**, *20*, 4887.

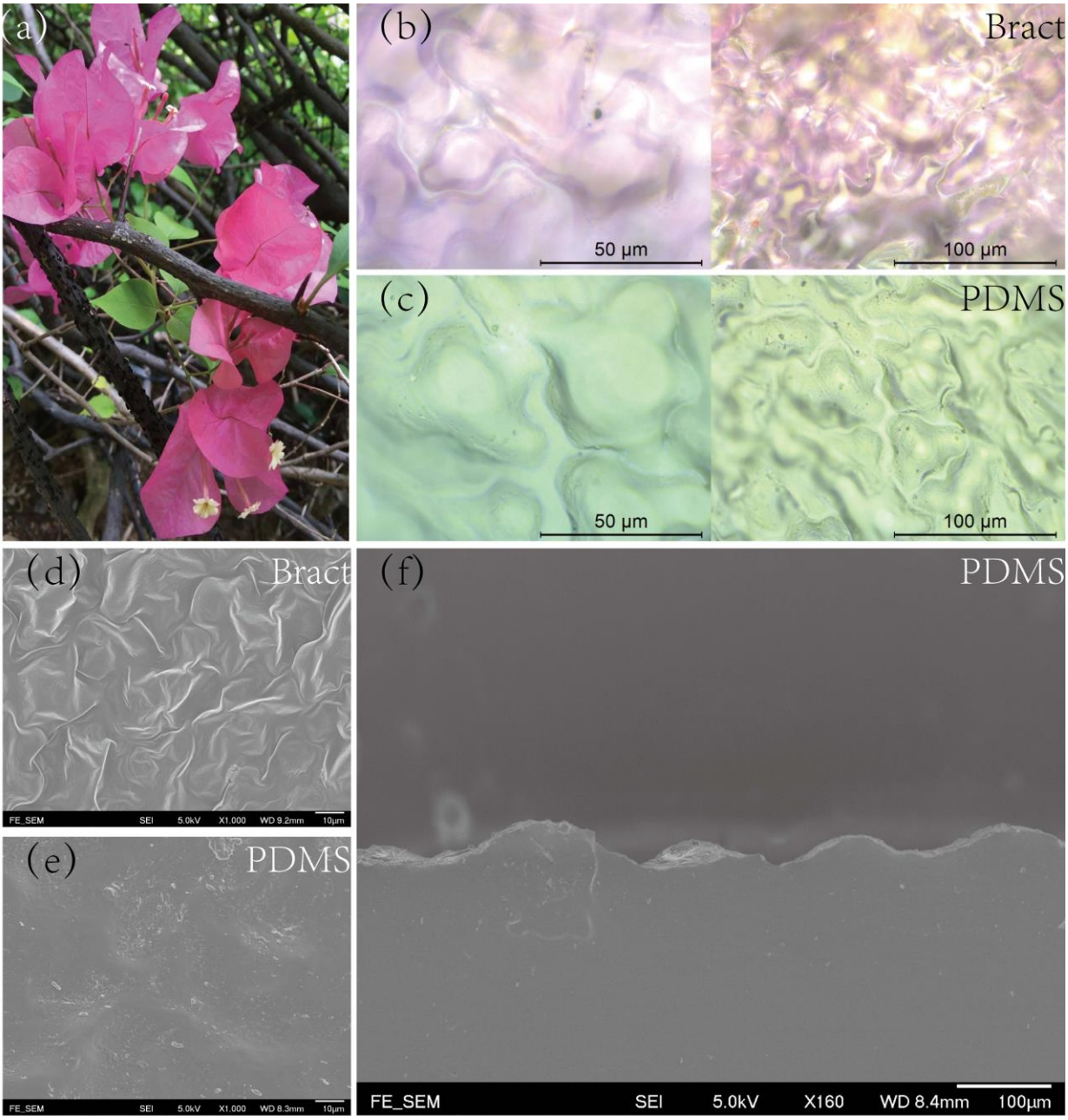


281

282 **Figure 1.** Characterizations of bract of bougainvillea glabra and molded PDMS surface. (a) Photo
283 of bougainvillea glabra; (b,c) Optical microscopy photos of bougainvillea glabra's bract and
284 molded PDMS surface; (d,e) Scanning electron microscopy (SEM) images of bougainvillea
285 glabra's bract and molded PDMS surface; (e) SEM cross-sectional view of a molded PDMS surface.

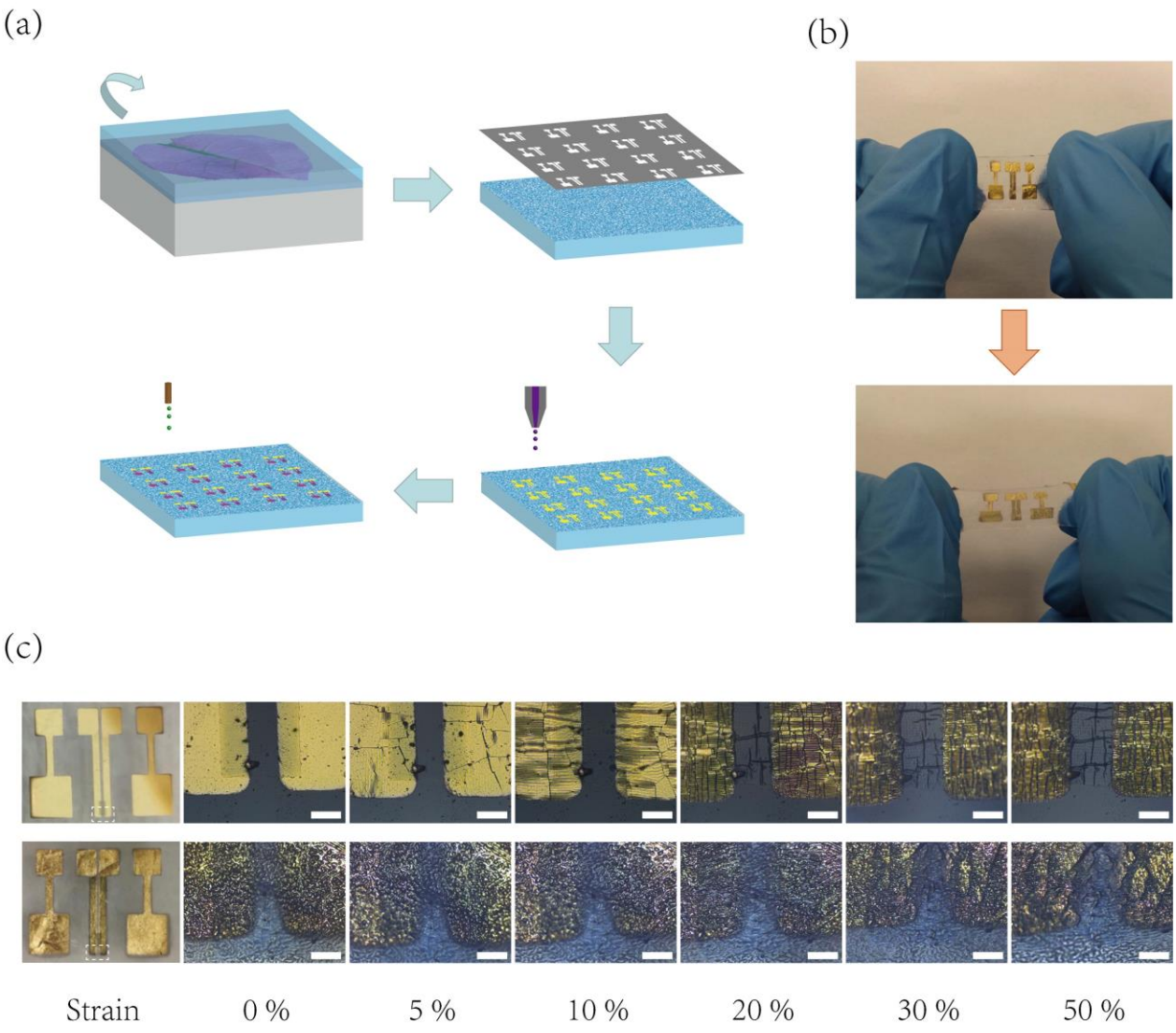


**Figure 2.** (a) Schematic illustration of the fabrication process of biomimicking stretchable OECTs. Up-left: mold PDMS out of bract; Up-right: deposit Au/Cr electrodes using shadow masking; Down-right: inkjet print channel and coating layer of PEDOT:PSS; Down-left: modify gate electrodes by drop casting; (b) Applying 50% strain to biomimicking stretchable OECT. (c) Morphology changes under increasing strains for control (up) and biomimicking (down) stretchable OECT. Dashed lines in the first column figures on the left indicate the positions where optical microscopy images presented on the right were taken. Scale bar: 200μm.

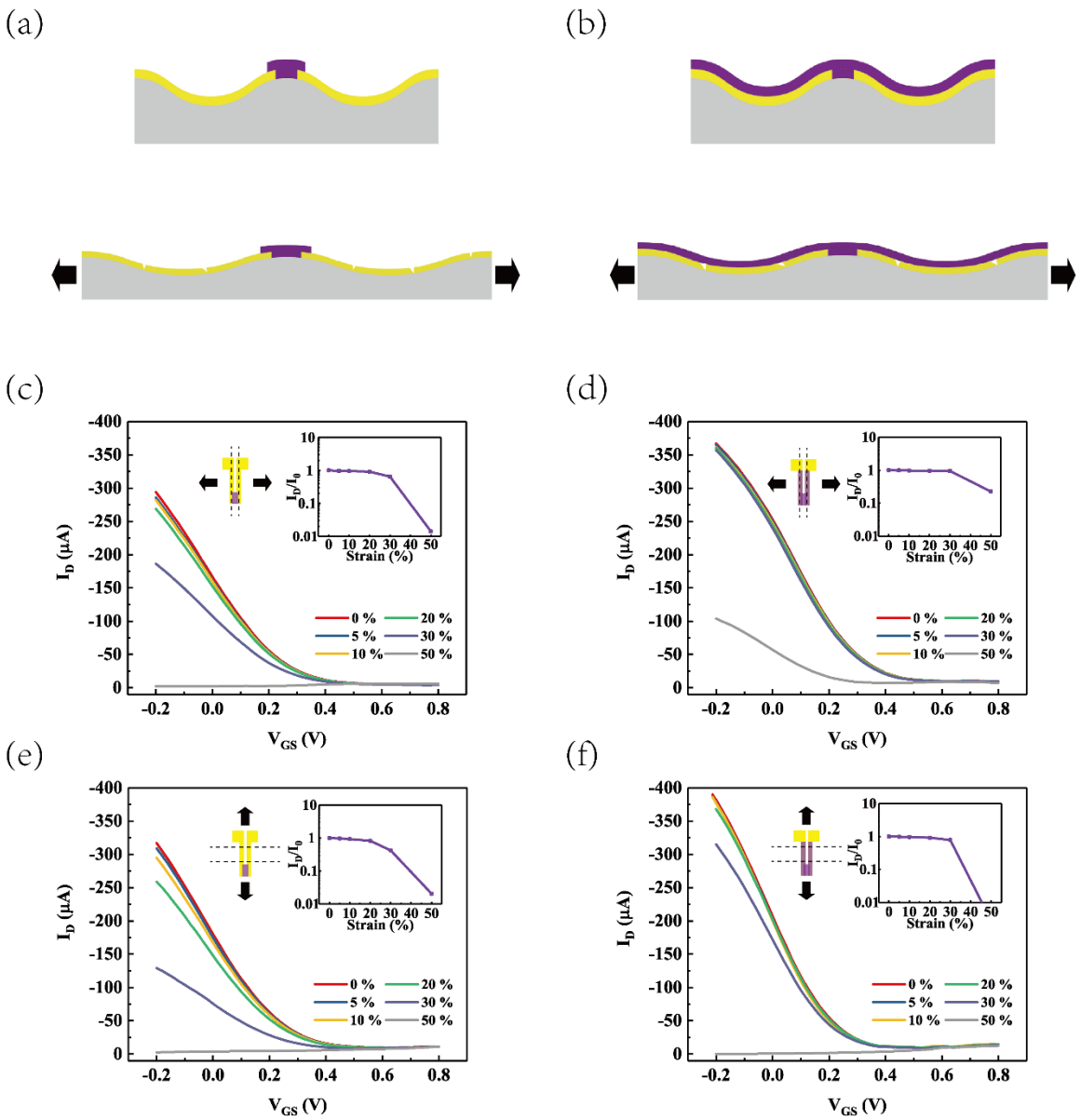


**Figure 3.** (a-b) Schematic illustration of structure differences for normal (left) and enhanced (right) biomimicking stretchable OECT. Dash lines indicate cracking. (c-f) Transfer characteristics ($V_{DS}$ = −0.1 V) of normal and enhanced biomimicking OECTs using Ag/AgCl gate electrode and PBS solution under omnidirectional strains, with the inset showing the relative current change when $V_{GS}$ = 0 V. Up-left: normal device under horizontal strains; Up-right: enhanced device under horizontal strains; Down-left: normal device under vertical strains, Down-right: enhanced device under vertical strains.

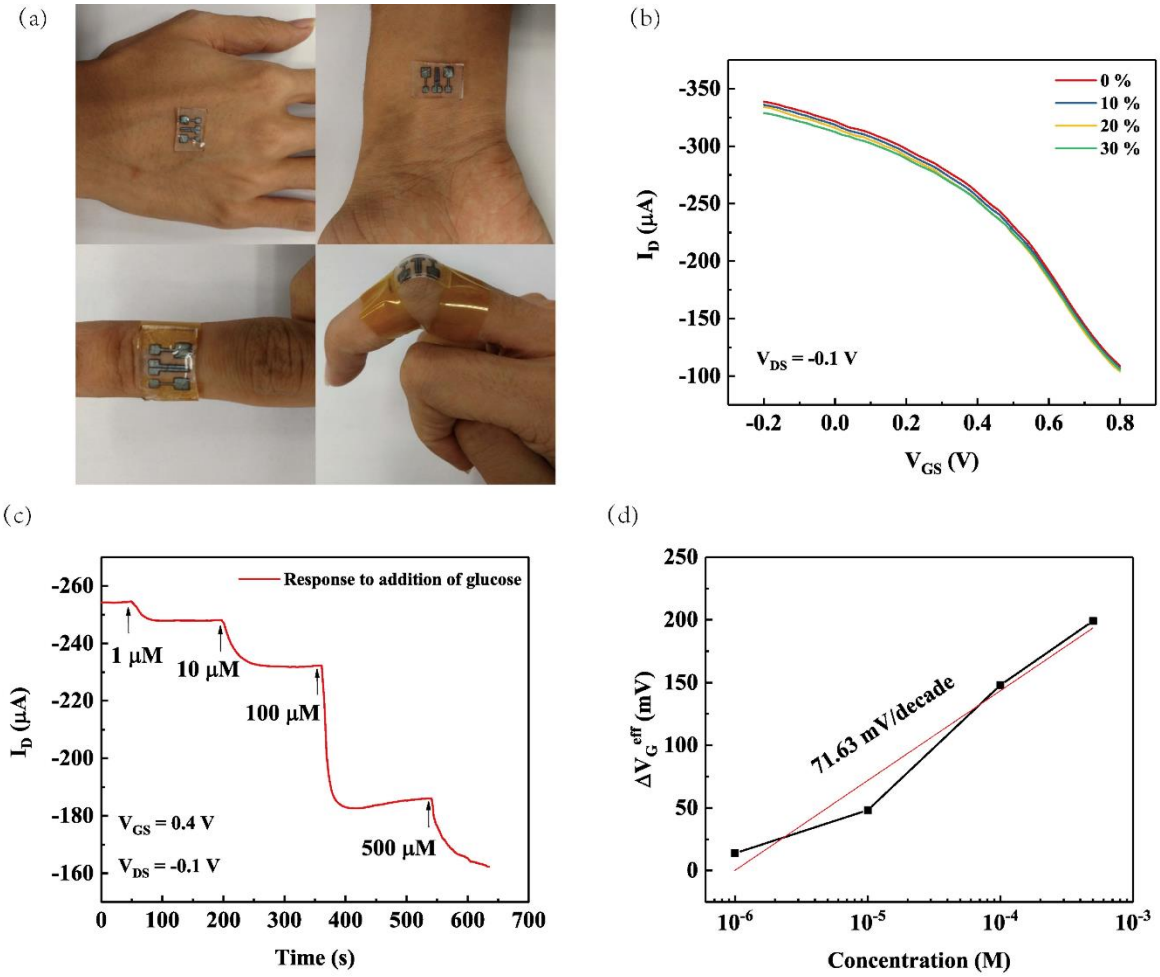


303

304 **Figure 4.** (a) Photographs of biomimicking OECTs as attachable devices; (b) Transfer
305 characteristics ($V_{DS}$ = −0.1 V) under 0%, 10%, 20%, 30% strains of a stretchable OECT with
306 Chitosan/Pt flakes & GOx/Au gate electrode ; (c) Channel current responses of a stretchable OECT
307 with Chitosan/Pt flakes & GOx/Au gate electrode to additions of glucose in PBS solution; (d) The
308 changes of effective gate voltage ($\Delta V_G^{eff}$) versus the glucose concentrations.

309

**The table of contents entry:**

**Stretchable** organic electrochemical transistors can find applications in wearable biomedical devices. This study develops a novel method to fabricate stretchable devices on biomimicking substrates based on bougainvillea glabra. The devices prepared by inkjet printing show stable performance with omnidirectional stretchability up to 30% and demonstrate the detection limit to glucose down to 1 μM.

**Keyword:** organic electrochemical transistor, flexible electronics, biomimicking, glucose detection

*Yuanzhe Li, Naixiang Wang, Anneng Yang, Haifeng Ling, Feng Yan**

**Biomimicking stretchable organic electrochemical transistor**